Facile Preparation of Ion-Imprinted Composite Film for Selective Electrochemical Removal of Nickel(II) Ions

Xiao Du,[†] Hao Zhang,[†] Xiaogang Hao,*[,†] Guoqing Guan,*[,‡] and Abuliti Abudula[‡]

[†]Department of Chemical Engineering, Taiyuan University of Technology, Taiyuan 030024, China
[‡]North Japan Research Institute for Sustainable Energy (NJRISE), Hirosaki University, 2-1-3, Matsubara, Aomori 030-0813, Japan

S *Supporting Information*

ABSTRACT: A facile unipolar pulse electropolymerization (UPEP) technique is successfully applied for the preparation of ion-imprinted composite film composed of ferricyanide-embedded conductive polypyrrole (FCN/PPy) for the selective electrochemical removal of heavy metal ions from wastewater. The imprinted heavy metal ions are found to be easily removed in situ from the growing film only by tactfully applying potential oscillation due to the unstable coordination of FCN to the imprinted ions. The obtained Ni^{2+} ion-imprinted FCN/PPy composite film shows fast uptake/release ability for the removal of Ni^{2+} ions from aqueous solution, and the adsorption equilibrium time is less than 50 s. The ion exchange capacity reaches 1.298 mmol g^{-1} and retains 93.5% of its initial value even after 1000 uptake/release cycles. Separation factors of 6.3, 5.6, and 6.2 for Ni^{2+}/Ca^{2+}, Ni^{2+}/K^+, and Ni^{2+}/Na^+, respectively, are obtained. These characteristics are attributed to the high identification capability of the ion-imprinted composite film for the target ions and the dual driving forces resulting from both PPy and FCN during the redox process. It is expected that the present method can be used for simple preparation of other ion-imprinted composite films for the separation and recovery of target heavy metal ions as well.

KEYWORDS: *heavy metal ions, selective removal, ion-imprinted, polypyrrole, ferricyanide*
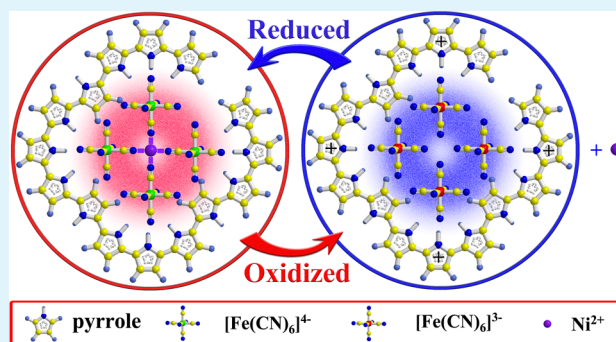
1. INTRODUCTION

Toxic heavy metal ion pollution has become a serious worldwide problem that endangers the environment and health of human beings.[1] Therefore, the efficient separation and recovery of industrial heavy metal ions from wastewater are of significant interest both from an environmental perspective and a resource perspective.[2] To date, various kinds of physical and chemical methods such as adsorption,[3,4] ion exchange,[5] chemical precipitation,[6] membrane separation,[7] and coagulation−flocculation[8] have been employed for this purpose. Among these methods, ion exchange and adsorption are considered the most practical method due to their simplicity, low cost, and reutilization.[5,9] However, the regeneration of ion exchangers and adsorbents always generates secondary waste from the chemical regenerates and the rinse water.

As an environmentally benign ion separation and recovery method, electrochemically switched ion exchange (ESIX) has attracted great attention in recent years.[10−15] In this method, the uptake and release of the target ions can be realized by modulating the redox states of the ESIX film, and the film can be repeatedly used. Thus, no secondary waste will be produced in this process.[10] In addition, ESIX can be applied to efficiently separate and recover target ions at very low concentration in the solution.[11] Inorganic metal hexacyanoferrate (MHCF) and organic conductive polymers (CPs) such as pyrrole (PPy),

polyaniline (PANI), and their derivatives are generally used as the ESIX materials. Among them, NiHCF and CuHCF films have been successfully formed on conductive substrates for the separation and removal of ^{137}Cs from radioactive liquid wastes.[11,12] Polypyrrole or polyaniline has been tailored as anion or cation exchangers by entrapping or doping of different counterions for the removal of F^-,[13] ClO_4^-,[10,14] and Ca^{2+} [15] from aqueous solutions. Nevertheless, this method was seldom applied for the selective separation of toxic heavy metal ions. Although some ESIX materials were developed for the removal of heavy metal ions from wastewater, the adsorbed heavy metal ions were difficult to be released from the materials by regulating the potential due to the strong intrinsic affinity of the chelating functional groups for the heavy metal ions.[16] According to the hard-soft-acids-bases (HSAB) theory,[17,18] the complexation ability of ferricyanide (FCN) in its oxidation state ($[Fe(CN)_6]^{3-}$) to some heavy metal ions, such as Ni^{2+}, Co^{2+}, and Zn^{2+}, is weaker than that of FCN in its reduction state ($[Fe(CN)_6]^{4-}$). Thus, if FCN serves as a counterion and is anchored to the PPy to fabricate a FCN/PPy composite film, the relatively strong complexation between $[Fe(CN)_6]^{4-}$ and

Scheme 1. Strategy for the Preparation of Ni²⁺-FCN/PPy Composite Film by Using the UPEP Method
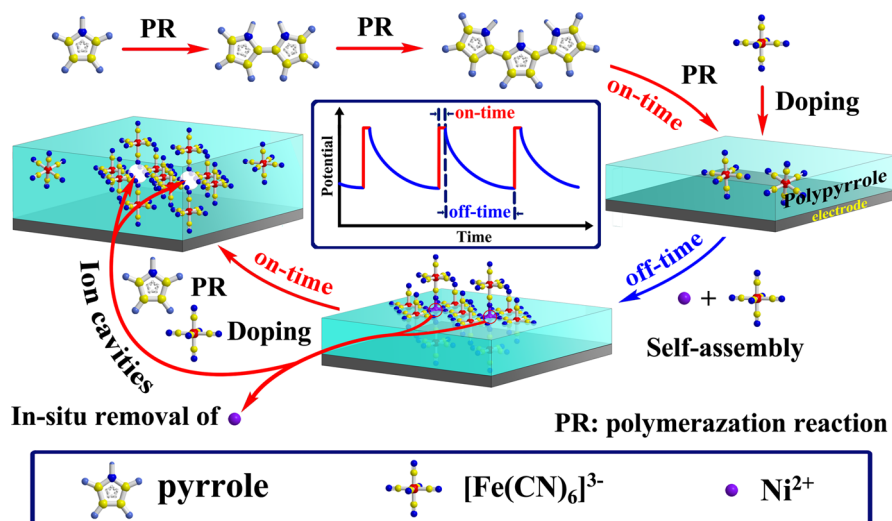
target ions will benefit the ion intercalation into the FCN/PPy film during the reduction process. Conversely, the adsorbed ion will be easily released due to the relative weak complexation of $[Fe(CN)_6]^{3-}$ to the target ions during the oxidation process. However, the anchored FCN in the FCN/PPy composite film was partially freed or flushed out of the film during the reduction process when the film was synthesized by using the traditional method.[19] Therefore, development of novel synthesis methods for such composite ESIX films is required.

The molecular or ion imprinting technique (MIT or IIT) is becoming a common and useful method for the selective recognition and separation of target molecules or ions from aqueous solutions.[20−22] The high adsorption capacity and excellent selectivity of ion-imprinted polymer (IIP) for the target ions can be achieved through the memory effect toward the target ions, which could be influenced by the interaction of the target ions with a specific ligand, coordination geometry, metal ion coordination number, charge, and size of the IIPs.[23,24] Recently, it was found that conducting IIP films can be formed on the electrode surface directly by in situ electropolymerization.[25] Therefore, it is possible to combine the IIP with ESIX material to create a novel hybrid film for highly selective removal of heavy metal ions from aqueous waste. In conventional IIP film preparations, the template ions have to be removed from the film subsequently by extensive washing steps after the electropolymerization due to the strong interaction between the template ions and the functional monomers.[23] In the present study, one of our main objectives is to find a way to eliminate the cumbersome washing steps during the fabrication of the ion-imprinted composite ESIX film using a facile strategy.

Nickel is a typical toxic heavy metal because inhalation of nickel and its compounds can lead to serious problems including nasopharynx and dermatological diseases and malignant tumors.[22,23] In this study, Ni²⁺ ions were selected as the target heavy metal ions. To fabricate Ni²⁺ ion-imprinted composite ESIX films, Ni²⁺, FCN, and PPy were used as template, complexing monomer, and conductive cross-linking agent, respectively. One-step unipolar pulse electropolymerization (UPEP) was applied to fabricate the objective Ni²⁺ ion-imprinted FCN-embedded PPy (Ni²⁺-FCN/PPy) film. It was expected that a stronger binding between the embedded FCN

and the PPy backbone could be generated and that the deintercalation of FCN from the growing PPy film could be restrained through the orientation of PPy main chains during the off-time period of the pulse cycle.[26−28] During the UPEP process, it is possible to maintain FCN in the oxidation state ($[Fe(CN)_6]^{3-}$) if a high potential (over 0.6 V) is applied on the working electrode.[29] Thus, due to the relatively weak complexation of $[Fe(CN)_6]^{3-}$ to Ni²⁺ based on the HSAB theory,[17] the imprinted Ni²⁺ ions can be easily removed in situ from the growing film by tactfully applying potential oscillation in the UPEP process. As a result, the extensive washing steps for the target ion in the conventional synthetic process could be eliminated. On the basis of this strategy, the objective Ni²⁺-FCN/PPy film was prepared and applied for the removal of Ni²⁺ ions in simulated wastewater. It is expected that such a one-step synthetic strategy will be a novel and promising way for the preparation of new types of ion-imprinted ESIX films for the selective separation of various toxic heavy metal ions from aqueous solution without producing any secondary effluents.

2. EXPERIMENTAL SECTION

2.1. Reagents and Instruments. Pyrrole (Sigma-Aldrich) was purified by distillation under reduced pressure and stored at low temperature in the dark under nitrogen atmosphere prior to use. Other chemicals were reagent grade and used without further purification. All solutions were prepared using ultrapure water (Millipore 18.2 MΩ cm).

Electrochemical preparation and characterization of the composite film were performed using a Potentiostat (Princeton Applied Research, VMP3, Oak Ridge, TN) controlled with EC-Lab software. A quartz crystal microbalance (Princeton Applied Research, QCM 922) was used to measure synchronously the mass change of composite film. Morphology of the composite film was examined with a scanning electron microscope (SEM) (LEO 438 VP, Carl Zeiss AG, Oberkochen, Germany). An energy dispersive X-ray spectroscopy (EDS) detection system built for the SEM instrument was used to detect the X-ray emission spectra of the samples. The X-ray photoelectron spectroscopy (XPS) scans were acquired with a VG Scientific ESCALab250i-XL unit (UK). Fourier transfer infrared spectroscopy (FT-IR) was recorded using an IRAffinity-1 workstation (Shimadzu, Japan).

2.2. Preparation of Ni²⁺-FCN/PPy Composite Film. Ni²⁺ ion-imprinted ferricyanide-embedded polypyrrole (Ni²⁺-FCN/PPy) composite film was fabricated by using the UPEP method in a freshly

prepared mixed solution containing 5 mmol L^{-1} pyrrole, 5 mmol L^{-1} $K_3Fe(CN)_6$, 5 mmol L^{-1} NiCl$_2$, 0.1 mol L^{-1} KCl, and 0.1 mol L^{-1} HCl. The UPEP process was performed using a three-electrode system in conjunction with a VMP3 Potentiostat. A 9 MHz At-cut, polished Pt-plated quartz crystal with 0.2 cm^2 of effective surface, a Pt sheet, and a saturated calomel electrode (SCE) served as the working electrode, counter electrode, and reference electrode, respectively. The whole electrochemical cell was immersed in a bath at a constant temperature of 10.0 °C. The pulse potential was set at 0.8 V with 10 ms on-time (t_{on}) and 100 ms off-time (t_{off}) during 20 000 cycles. The PPy without FCN embedding film and non-ion-imprinted FCN/PPy film were also fabricated using the same procedure in the solutions of 5 mmol L^{-1} pyrrole + 0.1 mol L^{-1} KCl + 0.1 mol L^{-1} HCl and 5 mmol L^{-1} pyrrole + 5 mmol L^{-1} $K_3Fe(CN)_6$ + 0.1 mol L^{-1} KCl+0.1 mol L^{-1} HCl, respectively. The composite films were fabricated on a Pt sheet (1.0 cm × 1.0 cm) in the same solution for the characterization of their morphologies and structures.

2.3. Characterization of Ni^{2+}-FCN/PPy Composite Film. After electropolymerization, the resulting film was washed with deionized water and then immersed in 0.1 M Ni(NO$_3$)$_2$ solution. Electrochemical characterization of the Ni^{2+}-FCN/PPy composite film was also performed using the three-electrode system. The ion exchange behavior of the film was investigated with cyclic voltammetry from −0.9 to 0.6 V at 25 mV s^{-1} under quiescent conditions. The electrochemical stability of the composite film was examined by alternately switching potential between reduction state (−0.2 V) and oxidation state (0.8 V) during 1000 cycles. Each stage of applied potential lasted for 50 s. The ion selectivity of Ni^{2+}-FCN/PPy composite film was tested in 0.1 mol L^{-1} Ni(NO$_3$)$_2$ solution, 0.1 mol L^{-1} Ca(NO$_3$)$_2$ solution, and a 0.1 mol L^{-1} solution mixture of Ni(NO$_3$)$_2$ and Ca(NO$_3$)$_2$ with a cation molar ratio of 1:1, respectively. Using the same procedure, the experiments on ion selectivity were also carried out in binary mixture solutions of Ni(NO$_3$)$_2$/KNO$_3$ and Ni(NO$_3$)$_2$/NaNO$_3$, respectively. To further investigate the relative selectivity of Ni^{2+} ion over other heavy metal ions, such as Co^{2+}, Zn^{2+}, Cd^{2+}, and Pb^{2+}, a simulated wastewater solution was examined containing 1.5 mmol L^{-1} each of Ni^{2+}, Co^{2+}, Zn^{2+}, Cd^{2+}, and Pb^{2+}. The detailed experimental method is shown in Supporting Information.

3. RESULTS AND DISCUSSION

A proposed schematic representation for the fabrication of the Ni^{2+} ion-imprinted FCN/PPy (Ni^{2+}-FCN/PPy) composite film by the UPEP method is illustrated in Scheme 1. The potential waveform of UPEP consists of a fixed potential during on-time followed by an open-circuit potential (OCP) decreasing over time during off-time. Initially, the pyrrole monomers at the electrode surface will be oxidized and polymerized to form the PPy film at 0.8 V during the short on-time period. Such a short pulse on-time period was found to produce fewer defects in the structure of the resulting PPy chains.[27,30] At this step, both FCN and Cl$^-$ in the electrolyte could be doped simultaneously into the structure of PPy as the counterions. Then, during the off-time period, the growing PPy chains are terminated by turning the current off.[26] Meanwhile, coordination reactions between Ni^{2+} ions in the electrolyte and the FCN embedded in the PPy occur. During the following on-time period of the pulse, the fresh pyrrole monomers will be continuously polymerized to form PPy film. According to the HSAB theory,[17,18] the coordination bonds between Ni^{2+} ions (served as borderline acids) and FCN (served as soft bases) should not be very strong, and thus, with the constant polymerization of positive pyrrole radicals on the surface of the film, Ni^{2+} ions bonded to the FCN could be removed easily from the growing composite film to the bulk solution under a strong positive potential such as 0.8 V. As a result, Ni^{2+} ion-imprinted cavities will be generated in composite film. As such, due to the

repetitive potential oscillation in the UPEP process, Ni^{2+} ion-imprinted ferricyanide-embedded polypyrrole (Ni^{2+}-FCN/PPy) composite film is expected to be fabricated.

3.1. Electropolymerization of the Ni^{2+}-FCN/PPy Composite Film. Following the above strategy, Ni^{2+}-FCN/PPy composite film was fabricated on the Pt-plated quartz crystal. The mass change occurring on the surface of the electrode was simultaneously measured by EQCM. As shown in Figure 1A, the mass change curve of the composite film shows a
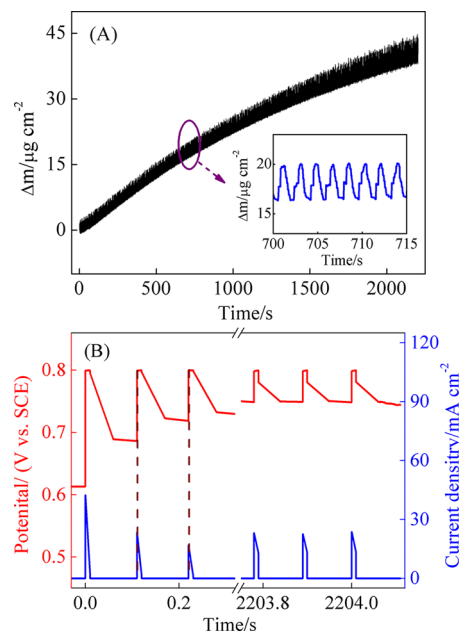

Figure 1. Mass change response (A) and potential/current density–time transients (B) recorded during the electropolymerization process for the formation of Ni^{2+}-FCN/PPy composite film.

fluctuating increasing trend, which indicates that the composite film is effectively synthesized on the electrode surface. Furthermore, the periodic decrease of mass reveals that there is an intermittent release of embedded ions from the composite film during the electropolymerization process. As shown in Figure S1A in Supporting Information, the one period of mass fluctuation corresponds to approximately 16 current pulses possibly because the release of imprinted ion needs stronger driving force, i.e., positive charge, from the accumulation of positive pyrrole radicals at the surface of the film. This phenomenon indicates that in situ polymerization of the composite film and in situ removal of the imprinted ions are taking place simultaneously. The current density/potential-time transients of the initial 0.32 s and the last 0.37 s during the UPEP are shown in Figure 1B. Herein, a fixed potential (0.8 V) was applied to generate current during the on-time period of the pulse (t_{on}: 10 ms) followed by a relaxation off-time period (t_{off}: 100 ms) without current being allowed to flow. With the applied potential during the on-time period, the electropolymerization of pyrrole monomers occurs on the substrate surface to form the PPy film. The generated current should be attributed to the Faradaic current from the oxidation of pyrrole monomers.[26] Then, during the off-time period, the polymerization reactions of pyrrole monomers are terminated due to the current being turned off. On the other hand, the coordination reactions between Ni^{2+} ions in the electrolyte and the FCN doped in the PPy film are simultaneously taking

place. Herein, a relatively long off-time period is set to improve the binding force between the PPy backbone and the embedded FCN through the rearrangement of PPy main chains with the fullest conjugation.[26,27] As shown in Figure S1B, Supporting Information, which shows the curves of open circuit potential (OCP) and peak current density versus the time during the UPEP process, the potential of the working electrode exceeds 0.6 V throughout the polymerization process. As such, the FCN should be maintained in the oxidation state ($[Fe(CN)_6]^{3-}$) and cannot be reduced to $[Fe(CN)_6]^{4-}$. In addition, the relatively shorter on-time period of 10 ms and lower reaction temperature of 10.0 °C are expected to slow down the electropolymerization rate of PPy main chains, which helps to restrain the excessive embedding of PPy for Ni^{2+} ions and FCN during the on-time period and reduce the defect density of PPy film.[26] Thus, the imprinted ions could be easily removed in situ from the composite film by tactfully applying potential oscillation due to the relatively weak coordination bond between Ni^{2+} ions and FCN in this case. In addition, the peak current density has an obvious fluctuation in the initial 100 s, which should be attributed to the two polymerization stages: in the first stage, the pyrrole monomers are polymerized to form FCN/PPy composite film on the Pt-plated quartz crystal, and in the second stage, the polymerization reaction of pyrrole monomers occurs only on the surface of the grown FCN/PPy film. The slight decrease of peak current density after 30 s is mainly due to the relatively higher resistance of the grown FCN/PPy film compared with that of the naked Pt substrate.

3.2. EDS Analysis. Elemental compositions of various films are identified and compared based on the EDS analysis. As shown in Figure 2, the PPy film is composed of elemental C, N,
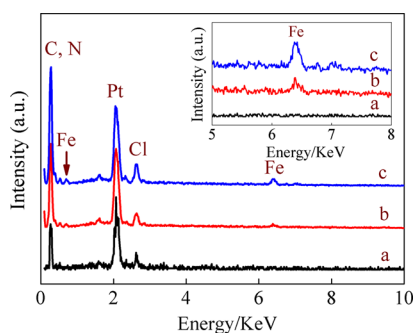

Figure 2. EDS spectra of PPy film (a), FCN/PPy film (b), and Ni^{2+}-FCN/PPy composite film (c); the inset is an enlargement of the EDS spectra.

and Cl, but in the FCN/PPy and Ni^{2+}-FCN/PPy films, elemental Fe is also observed. This indicates that both FCN and Cl ions are embedded into the PPy film. Interestingly, no Ni peak is found in the spectrum of the as-prepared Ni^{2+}-FCN/PPy film, indicating that Ni^{2+} ions have been removed from the film during the electrodeposition process as expected.

3.3. FT-IR Analysis. FT-IR spectra of the PPy and Ni^{2+}-FCN/PPy films are shown in Figure 3. Similar absorption peaks from 1030 to 1540 cm^{-1}, which are the typical characteristic peaks of PPy, are detected for both films. In the spectra, the peaks located around 1540 and 1460 cm^{-1} correspond to the symmetric and asymmetric pyrrole ring stretching modes, respectively.[31] The peak centered at 1290 cm^{-1} corresponds to the in-plane vibration of =C−H.[31] The stretching frequency at
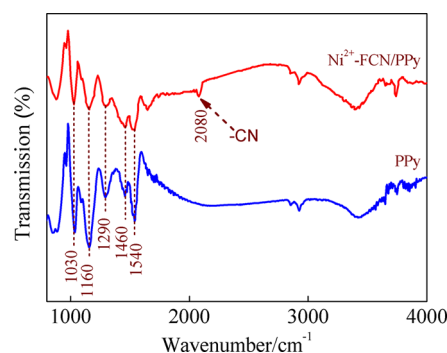

Figure 3. FT-IR spectra of PPy and Ni^{2+}-FCN/PPy films.

1160 cm^{-1} is attributed to the C−N stretching vibration, and the absorption peak at 1030 cm^{-1} is due to N−H bending vibration.[31,32] Herein, an obvious absorption peak at 2080 cm^{-1}, which is assigned to the stretching vibration of the C≡N group in the cyanometalate lattice of FCN,[33] is found in the spectrum of the Ni^{2+}-FCN/PPy film, indicating that FCN has been successfully embedded into the Ni^{2+}-FCN/PPy film.

3.4. SEM Analysis. SEM images of the fabricated PPy and FCN/PPy films are shown in Figure 4, parts A and B,
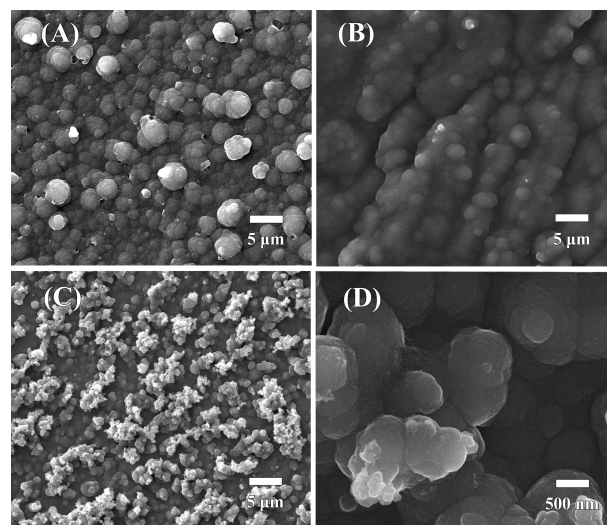

Figure 4. SEM images of PPy (A), FCN/PPy (B), and Ni^{2+}-FCN/PPy (C, D) films.

respectively. Both films exhibit a typical cauliflower-like morphology structure. However, for the Ni^{2+}-FCN/PPy film, as shown in Figure 4, parts C and D, it is obvious that porous and globular grains are formed. Such structures could provide more surface area for the uptake and release of ions.

3.5. ESIX Characterization of Ni^{2+}-FCN/PPy Composite Film. Figure 5, parts A and B, shows typical cyclic voltammograms (CV) and massograms of the FCN/PPy film and Ni^{2+}-FCN/PPy composite film in 0.1 M $Ni(NO_3)_2$ solution, respectively. As shown in Figure 5A, the mass of FCN/PPy film changes a little during the redox process. Although it is reported that the FCN in the FCN/PPy film could be flushed out from the film during the reduction process at a potential more negative than −0.4 V (vs SCE) when the film was prepared by another method,[19] a decline in the mass of FCN/PPy film prepared by the present method is not observed. It is possible that a stronger binding force between
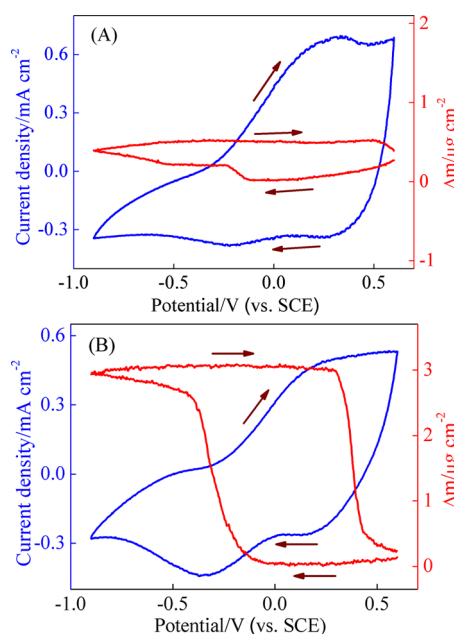
Figure 5. Cyclic voltammograms and massograms of FCN/PPy film (A) and Ni^{2+}-FCN/PPy composite film (B) in 0.1 mol L^{-1} Ni(NO$_3$)$_2$ solution at a scan rate of 25 mV s^{-1}.

the PPy backbone and FCN could be generated by the orientation of PPy main chains during the off-time period when the UPEP method was used for the film preparation.[26,27] In contrast, as shown in Figure 5B, there is a significant mass change for the Ni^{2+}-FCN/PPy composite film during the redox process. The mass of Ni^{2+}-FCN/PPy film increases rapidly when sweeping the potential in the negative direction from 0 to −0.9 V. It should be attributed to the insertion of Ni^{2+} ions into the film according to the charge compensation mechanism.[34] On the contrary, when the potential is reversed to the positive direction, a steep decline in the mass change starts from 0.3 to 0.6 V. This should correspond to the release of Ni^{2+} ions. The intercalation and release of the Ni^{2+} ions occurring at different potentials should be attributed to the different complexation abilities of FCN to Ni^{2+} ions in its oxidation state ([Fe(CN)$_6$]$^{3-}$) and reduction state ([Fe(CN)$_6$]$^{4-}$). As stated above, according to the HASB theory,[17,18] the complexation of [Fe(CN)$_6$]$^{4-}$ to Ni^{2+} is generally stronger than that of [Fe(CN)$_6$]$^{3-}$. Hence, when the composite film is in the oxidized state, Ni^{2+} ions are easily excluded from the film. Herein, compared with the non-ion-imprinted FCN/PPy film, the Ni^{2+}-FCN/PPy composite film shows much superior ion exchange property for Ni^{2+} ions, which is mainly attributed to the high surface area and a large number of ion-imprinted cavities in the film.

The effect of Ni^{2+} ion concentration in the aqueous solution on the adsorption property of Ni^{2+}-FCN/PPy composite film is also investigated. The amount of Ni^{2+} ions adsorbed per unit mass of film increases with the initial concentration of Ni^{2+} ion in the solution at first, and then a saturation adsorption is reached soon when the initial concentration exceeds 0.02 mol L^{-1} (as shown in Figure S2, Supporting Information). Furthermore, as shown in Figure S3, Supporting Information, the adsorption capacity of Ni^{2+}-FCN/PPy composite film is reduced with a decrease in pH of the aqueous solution, which should be due to Ni^{2+} ion-imprinted sites of the polymer being

occupied by protons rather than Ni^{2+} ions themselves in the acid environment.

3.6. Selectivity of Ni^{2+}-FCN/PPy Composite Film. The relative selectivity of Ni^{2+}-FCN/PPy composite film is investigated by competitive adsorption of Ni^{2+}/Ca^{2+}, Ni^{2+}/K$^+$ and Ni^{2+}/Na$^+$ from their binary mixtures. The CVs and mass change responses measured simultaneously in 0.1 mol L^{-1} Ni(NO$_3$)$_2$ solution, 0.1 mol L^{-1} Ca(NO$_3$)$_2$ solution, and 0.1 mol L^{-1} mixture solution of Ni(NO$_3$)$_2$ and Ca(NO$_3$)$_2$, respectively, for Ni^{2+}-FCN/PPy composite film are shown Figure S4, parts A and B, Supporting Information, respectively. Herein, the reproducible CV and mass change signals are obtained after the 5th scan in each case. That is, the 6th cycle of each experiment is chosen as the representative behavior observed. As shown in Figure S4, parts A and B, Supporting Information, the Ni^{2+}-FCN/PPy composite film tested in Ni(NO$_3$)$_2$ solution shows larger peak current density and more mass change within the same potential range than those in Ca(NO$_3$)$_2$ solution. This indicates that the Ni^{2+}-FCN/PPy composite film has much superior electroactivity in the aqueous solution containing Ni^{2+} ions. To further quantitatively evaluate the relative selectivity of Ni^{2+}-FCN/PPy composite film for various cations, selective experiments are also carried out using the binary mixture solutions of Ni(NO$_3$)$_2$/KNO$_3$ and Ni-(NO$_3$)$_2$/NaNO$_3$, respectively, and the separation factors are calculated (the detailed calculation methods are shown in Supporting Information). Table 1 summarizes the calculated

Table 1. Separation Factors of Ni^{2+}-FCN/PPy Film in 0.1 mol L^{-1} Binary Mixture Solutions

	M_{Ni}'	M'	$\Delta m_{mix} \cdot F/Q_{mix}$	α
Ni^{2+}/Ca^{2+}	70.7 ± 0.8	43.6 ± 0.5	33.5 ± 0.5	6.3 ± 0.8
Ni^{2+}/K$^+$	70.7 ± 0.8	39.6 ± 0.6	35.7 ± 0.5	5.6 ± 0.7
Ni^{2+}/Na$^+$	70.7 ± 0.8	25.3 ± 0.5	34.6 ± 0.6	6.2 ± 0.6

apparent molar weights of cations and separation factors of the composite film, both of which are the average values of the last five (of ten) redox cycles. Herein, if it is considered that during the redox cycling, one mole of redox site is converted and electroneutrality is maintained strictly by the cations present in the solution, the apparent molar weight (M') should be equal to the molecular weight of the target cation. However, as shown in Table 1, all the values obtained for the apparent molar weights (M') are higher than those of the corresponding cations. A possible explanation for this discrepancy would be the migration of solvent into or out of the film at the same time as the cations are taken up or released to balance the generated charges. Furthermore, all the separation factors for Ni^{2+}/Ca^{2+}, Ni^{2+}/K$^+$, and Ni^{2+}/Na$^+$ are much larger than 1, indicating that the binding of Ni^{2+}-FCN/PPy composite film to Ni^{2+} ions is much stronger than that to Ca^{2+}, K$^+$, and Na$^+$ ions. Such an excellent selectivity to Ni^{2+} ions should result from the polymer memory effects toward target ion interaction with a specific ligand, metal ion coordination number, charge, and size. This is the typical characteristic of ion-imprinted materials. Furthermore, Table S1, Supporting Information, indicates that Ni^{2+} can be also selectively absorbed by Ni^{2+}-FCN/PPy composite film when other heavy metal ions such as Co^{2+}, Zn^{2+}, Cd^{2+}, and Pb^{2+} coexisted with it in aqueous solution.

3.7. Dynamic Characteristics of Ni^{2+}-FCN/PPy Composite Film. To simulate the repeated uptake/release of Ni^{2+} ions from aqueous solution using the Ni^{2+}-FCN/PPy composite

film, periodically switching of the redox state of the film in 0.1 mol L^{-1} $Ni(NO_3)_2$ solution is performed and the mass change of the film is recorded during the redox process. Figure 6 shows
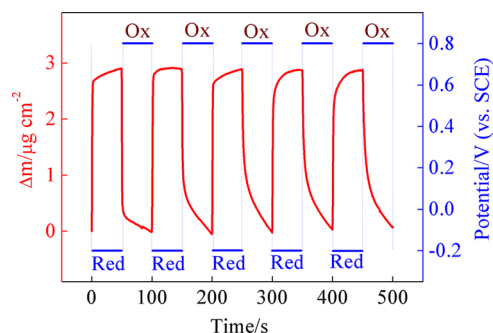

Figure 6. Massograms of Ni^{2+}-FCN/PPy composite film between the reduced state (−0.2 V) and the oxidized state (0.8 V) in 0.1 mol L^{-1} $Ni(NO_3)_2$.

the typical ion uptake/release property with alternately regulating the potential between the reduction state (−0.2 V) and the oxidation state (0.8 V). As shown in Figure 6, the mass of Ni^{2+}-FCN/PPy film is increased during the reduction process and then decreased during the oxidation process. The observed mass change should be related to the uptake/release of the cations according to the charge compensation mechanism. In this study, EDS and XPS analysis is also used to characterize the composition of Ni^{2+}-FCN/PPy composite film in the reduction and oxidation states. As shown in Figure S5, Supporting Information, absorption peaks of Ni obviously appear when the film is in the reduction state while the peaks disappear in the oxidation state. The same results were observed from the XPS spectra of the composite shown in Figure S6, Supporting Information. This further indicates that electrochemically controlled intercalation and release of the Ni^{2+} ions can be realized via switching the redox states of the composite film. Herein, it should be noted that the adsorption equilibrium time of Ni^{2+} ions on the composite film is less than 50 s. Such a high adsorption rate of Ni^{2+}-FCN/PPy composite film, compared with other IIPs shown in Table S2, Supporting Information, is mainly attributed to the following two reasons. (i) During the ESIX process, electricity is a main driving force for the uptake/release of ions, besides physical and chemical adsorptions; (ii) PPy and FCN can provide a dual-driving force for the uptake/release of Ni^{2+} ions and exert a synergetic effect for the ion adsorption. In this study, the equilibrium absorption capacity of the composite film for Ni^{2+} ions reaches 1.298 mmol g^{-1}, which is a relatively high value among the Ni^{2+}-imprinted IIPs shown in Table S2, Supporting Information.

3.8. Cycle Stability of Ni^{2+}-FCN/PPy Composite Film.
To assess the stability of as-prepared Ni^{2+}-FCN/PPy composite film, the change in the ion exchange capacity is further investigated by periodically switching redox states of composite film over a large number of cycles. Figure 7 shows the change in normalized ion exchange capacity and desorption efficiency as a function of the cycle number in 0.1 mol L^{-1} $Ni(NO_3)_2$ solution. The ion exchange capacity of Ni^{2+}-FCN/PPy composite film retains 93.5% of its initial value even after 1000 cycles, and the desorption efficiency of Ni^{2+} ions in each ion exchange process maintains above 98.5%. These results indicate that the Ni^{2+}-FCN/PPy composite film can serve as an excellent ESIX
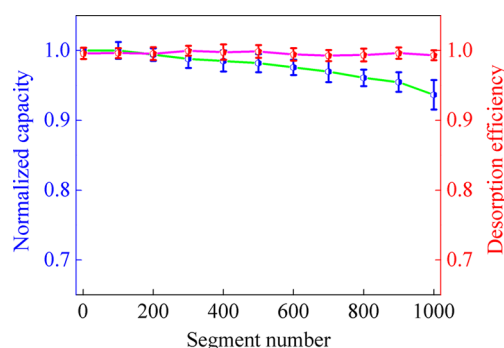

Figure 7. Change in normalized ion exchange capacity and desorption efficiency as a function of the cycle number in 0.1 mol L^{-1} $Ni(NO_3)_2$ solution over 1000 cycles.

material for the separation and recovery of Ni^{2+} ions from aqueous solution.

■ ASSOCIATED CONTENT

Ⓢ Supporting Information
(1) The detailed calculation method for separation factors; (2) the mass/current density transients during the UPEP of composite film; (3) the effect of Ni^{2+} ion initial concentration on the adsorption quantity of composite film; (4) the effect of pH value on the adsorption quantity of composite film; (5) simultaneous CV (A) and EQCM (B) curves of Ni^{2+}-FCN/PPy composite film in 0.1 mol L^{-1} $Ni(NO_3)_2$ solution; (6) the relative selectivity of Ni^{2+}-FCN/PPy composite film for Ni^{2+} ion with respect to other heavy metal ions; (7) EDS spectra of Ni^{2+}-FCN/PPy composite film; (8) XPS spectra of Ni^{2+}-FCN/PPy composite film; (9) separation characteristics of different ion-imprinted polymers for Ni^{2+} ion. This material is available free of charge via the Internet at http://pubs.acs.org.

■ AUTHOR INFORMATION

Corresponding Authors
*Phone: +86 3516018193; fax: +86 3516018554; e-mail: xghao@tyut.edu.cn; tyutxghao@hotmail.com (X.H.).
*Phone: +81 177627756; fax: +81 177355411; e-mail: guan@cc.hirosaki-u.ac.jp (G.G.).

Notes
The authors declare no competing financial interest.

■ ACKNOWLEDGMENTS

■ REFERENCES

(1) Godfray, H. C. J.; Beddington, J. R.; Crute, I. R.; Haddad, L.; Lawrence, D.; Muir, J. F.; Pretty, J.; Robinson, S.; Thomas, S. M.; Toulmin, C. Food Security: The Challenge of Feeding 9 Billion People. *Science* **2010**, *327*, 812−818.
(2) Poliakoff, M.; Fitzpatrick, J. M.; Farren, T. R.; Anastas, P. T. Green Chemistry: Science and Politics of Change. *Science* **2002**, *297*, 807−810.
(3) Kim, E.-J.; Lee, C.-S.; Chang, Y.-Y.; Chang, Y.-S. Hierarchically Structured Manganese Oxide-Coated Magnetic Nanocomposites for the Efficient Removal of Heavy Metal Ions from Aqueous Systems. *ACS Appl. Mater. Interfaces* **2013**, *5*, 9628−9634.

(4) Zhang, Q.; Wang, N.; Zhao, L.; Xu, T.; Cheng, Y. Polyamido-amine Dendronized Hollow Fiber Membranes in the Recovery of Heavy Metal Ions. *ACS Appl. Mater. Interfaces* **2013**, *5*, 1907−1912.

(5) Chen, Y.; Pan, B.; Li, H.; Zhang, W.; Lv, L.; Wu, J. Selective Removal of Cu(II) Ions by Using Cation-Exchange Resin-Supported Polyethyleneimine (PEI) Nanoclusters. *Environ. Sci. Technol.* **2010**, *44*, 3508−3513.

(6) Fu, F.; Xie, L.; Tang, B.; Wang, Q.; Jiang, S. Application of a Novel Strategy—Advanced Fenton-Chemical Precipitation to the Treatment of Strong Stability Chelated Heavy Metal Containing Wastewater. *Chem. Eng. J.* **2012**, *189−190*, 283−287.

(7) Wang, R.; Guan, S.; Sato, A.; Wang, X.; Wang, Z.; Yang, R.; Hsiao, B. S.; Chu, B. Nanofibrous Microfiltration Membranes Capable of Removing Bacteria, Viruses and Heavy Metal Ions. *J. Membr. Sci.* **2013**, *446*, 376−382.

(8) Beltrán Heredia, J.; Sánchez Martín, J. Removing Heavy Metals from Polluted Surface Water with a Tannin-Based Flocculant Agent. *J. Hazard. Mater.* **2009**, *165*, 1215−1218.

(9) Hadi, P.; Barford, J.; McKay, G. Toxic Heavy Metal Capture Using a Novel Electronic Waste-Based Material—Mechanism, Modeling and Comparison. *Environ. Sci. Technol.* **2013**, *47*, 8248−8255.

(10) Lin, Y.; Cui, X.; Bontha, J. Electrically Controlled Anion Exchange Based on Polypyrrole and Carbon Nanotubes Nanocomposite for Perchlorate Removal. *Environ. Sci. Technol.* **2006**, *40*, 4004−4009.

(11) Sun, B.; Hao, X.; Wang, Z.; Guan, G.; Zhang, Z.; Li, Y.; Liu, S. Separation of Low Concentration of Cesium Ion from Wastewater by Electrochemically Switched Ion Exchange Method: Experimental Adsorption Dinetics Analysis. *J. Hazard. Mater.* **2012**, *233-234*, 177−183.

(12) Chen, R.; Tanaka, H.; Kawamoto, T.; Asai, M.; Fukushima, C.; Kurihara, M.; Ishizaki, M.; Watanabe, M.; Arisaka, M.; Nankawa, T. Thermodynamics and Mechanism Studies on Electrochemical Removal of Cesium Ions from Aqueous Solution Using a Nanoparticle Film of Copper Hexacyanoferrate. *ACS Appl. Mater. Interfaces* **2013**, *5*, 12984−12990.

(13) Cui, H.; Li, Q.; Qian, Y.; Tang, R.; An, H.; Zhai, J. Defluoridation of Water Via Electrically Controlled Anion Exchange by Polyaniline Modified Electrode Reactor. *Water Res.* **2011**, *45*, 5736−5744.

(14) Zhang, S.; Shao, Y.; Liu, J.; Aksay, I. A.; Lin, Y. Graphene−Polypyrrole Nanocomposite as a Highly Efficient and Low Cost Electrically Switched Ion Exchanger for Removing $ClO^{4−}$ from Wastewater. *ACS Appl. Mater. Interfaces* **2011**, *3*, 3633−3637.

(15) Weidlich, C.; Mangold, K.-M. Electrochemically Switchable Polypyrrole Coated Membranes. *Electrochim. Acta* **2011**, *56*, 3481−3484.

(16) Omraei, M.; Esfandian, H.; Katal, R.; Ghorbani, M. Study of the Removal of Zn(II) from Aqueous Solution Using Polypyrrole Nanocomposite. *Desalination* **2011**, *271*, 248−256.

(17) Karmarkar, S. V. Anion-Exchange Chromatography of Metal Cyanide Complexes with Gradient Separation and Direct UV Detection. *J. Chromatogr., A* **2002**, *956*, 229−235.

(18) Pearson, R. G. Hard and Soft Acids and Bases. *J. Am. Chem. Soc.* **1963**, *85*, 3533−3539.

(19) Torres-Gómez, G.; Gómez-Romero, P. Conducting Organic Polymers with Electroactive Dopants. Synthesis and Electrochemical Properties of Hexacyanoferrate-Doped Polypyrrole. *Synth. Met.* **1998**, *98*, 95−102.

(20) Luo, X.; Deng, F.; Min, L.; Luo, S.; Guo, B.; Zeng, G.; Au, C. Facile One-Step Synthesis of Inorganic-Framework Molecularly Imprinted TiO_2/WO_3 Nanocomposite and Its Molecular Recognitive Photocatalytic Degradation of Target Contaminant. *Environ. Sci. Technol.* **2013**, *47*, 7404−7412.

(21) Preetha, C. R.; Gladis, J. M.; Rao, T. P.; Venkateswaran, G. Removal of Toxic Uranium from Synthetic Nuclear Power Reactor Effluents Using Uranyl Ion Imprinted Polymer Particles. *Environ. Sci. Technol.* **2006**, *40*, 3070−3074.

(22) Singh, D. K.; Mishra, S. Synthesis, Characterization and Analytical Applications of Ni(II)-Ion Imprinted Polymer. *Appl. Surf. Sci.* **2010**, *256*, 7632−7637.

(23) Vatanpour, V.; Madaeni, S. S.; Zinadini, S.; Rajabi, H. R. Development of Ion Imprinted Technique for Designing Nickel Ion Selective Membrane. *J. Membr. Sci.* **2011**, *373*, 36−42.

(24) Arbab-Zavar, M. H.; Chamsaz, M.; Zohuri, G.; Darroudi, A. Synthesis and Characterization of Nano-pore Thallium (III) Ion-Imprinted Polymer as a New Sorbent for Separation and Preconcentration of Thallium. *J. Hazard. Mater.* **2011**, *185*, 38−43.

(25) Ameli, A.; Alizadeh, N. Nanostructured Conducting Molecularly Imprinted Polymer for Selective Uptake/Release of Naproxen by the Electrochemically Controlled Sorbent. *Anal. Biochem.* **2012**, *428*, 99−106.

(26) Du, X.; Hao, X.; Wang, Z.; Ma, X.; Guan, G.; Abuliti, A.; Ma, G.; Liu, S. Highly Stable Polypyrrole Film Prepared by Unipolar Pulse Electro-polymerization Method as Electrode for Electrochemical Supercapacitor. *Synth. Met.* **2013**, *175*, 138−145.

(27) Sharma, R. K.; Rastogi, A. C.; Desu, S. B. Pulse Polymerized Polypyrrole Electrodes for High Energy Density Electrochemical Supercapacitor. *Electrochem. Commun.* **2008**, *10*, 268−272.

(28) Wang, Z.; Wang, Y.; Hao, X.; Liu, S.; Guan, G.; Abudula, A. An All Cis-Polyaniline Nanotube Film: Facile Synthesis and Applications. *Electrochim. Acta* **2013**, *99*, 38−45.

(29) Hao, X.; Yan, T.; Wang, Z.; Liu, S.; Liang, Z.; Shen, Y.; Pritzker, M. Unipolar Pulse Electrodeposition of Nickel Hexacyanoferrate Thin Films with Controllable Structure on Platinum Substrates. *Thin Solid Films* **2012**, *520*, 2438−2448.

(30) Davies, A.; Audette, P.; Farrow, B.; Hassan, F.; Chen, Z.; Choi, J.-Y.; Yu, A. Graphene-Based Flexible Supercapacitors: Pulse-Electro-polymerization of Polypyrrole on Free-Standing Graphene Films. *J. Phys. Chem. C* **2011**, *115*, 17612−17620.

(31) He, C.; Yang, C. H.; Li, Y. F. Chemical Synthesis of Coral-like Nanowires and Nanowire Networks of Conducting Polypyrrole. *Synth. Met.* **2003**, *139*, 539−545.

(32) Yang, P.; Zhang, J.; Guo, Y. Synthesis of Intrinsic Fluorescent Polypyrrole Nanoparticles by Atmospheric Pressure Plasma Polymerization. *Appl. Surf. Sci.* **2009**, *255*, 6924−6929.

(33) Chen, W.; Xia, X. H. Highly Stable Nickel Hexacyanoferrate Nanotubes for Electrically Switched Ion Exchange. *Adv. Funct. Mater.* **2007**, *17*, 2943−2948.

(34) Akieh, M. N.; Price, W. E.; Bobacka, J.; Ivaska, A.; Ralph, S. F. Ion Exchange Behaviour and Charge Compensation Mechanism of Polypyrrole in Electrolytes Containing Mono-, Di- and Trivalent Metal Ions. *Synth. Met.* **2009**, *159*, 2590−2598.